



# Study on the formation of photoactive species in $\text{XPMo}_{12-n}\text{V}_n\text{O}_{40-}$ -HCl system and its effect on photocatalysis oxidation of cyclohexane by dioxygens under visible light irradiation

Senpei Tang<sup>a</sup>, Jialuo She<sup>b</sup>, Zaihui Fu<sup>a,\*</sup>, Shenyi Zhang<sup>a</sup>, Zeyu Tang<sup>a</sup>, Chao Zhang<sup>a</sup>, Yachun Liu<sup>a</sup>, Dulin Yin<sup>a</sup>, Jianwei Li<sup>b</sup>

<sup>a</sup> National & Local United Engineering Laboratory for New Petrochemical Materials & Fine Utilization of Resources, Key Laboratory of Resource Fine-Processing and Advanced Materials of Hunan Province and Key Laboratory of Chemical Biology and Traditional Chinese Medicine Research (Ministry of Education of China), College of Chemistry and Chemical Engineering, Hunan Normal University, Changsha 410081, China

<sup>b</sup> State Key Laboratory of Chemical Resource Engineering, Beijing University of Chemical Technology, Beijing 100029, China



## ARTICLE INFO

### Article history:

Received 15 January 2017

Received in revised form 26 March 2017

Accepted 7 May 2017

Available online 11 May 2017

### Keywords:

Vanadium-substituted molybdochosphoric acids/salts

Photo-catalytic oxidation

Cyclohexane

Cyclohexanol

Cyclohexanone

Visible light

## ABSTRACT

The formation of photoactive species in the Keggin-type  $\text{XPMo}_{12-n}\text{V}_n\text{O}_{40-}$  polyoxometalates (POMs,  $n = 1-3$ ,  $\text{X} = \text{H}^+$ , tetramethyl (TMA), tetrabutyl (TBA) or cetyltrimethyl (CTMA) ammonium cation ( $\text{Q}^+$ ))-HCl system was researched in details by UV-vis and its photo-catalysis performance evaluated via the oxidation of cyclohexane by dioxygens ( $\text{O}_2$ ) in acetonitrile (MeCN) under visible light irradiation. The results showed that the  $\text{V}^{\text{IV}}\text{-O-M}$  ( $\text{M}$  for  $\text{V}^{\text{IV}}$  or  $\text{Mo}^{\text{IV}}$ ) sites of POM can capture HCl to form a protonated photoactive species (PA,  $\text{POM}\text{-}(\text{V}^{\text{IV}}\text{OHM})^+\text{Cl}^-$ ) and the solvent MeCN likely participates the formation of such PA species via weak coordination. This PA species, with a characteristic absorption band of 475 nm, a  $^{51}\text{V}$ -NMR chemical shift of  $-550$  ppm and an oxidative potential of higher than  $0.9$  V, should be responsible for the present photo-catalysis oxidation. The formation of PA species was accelerated significantly with increasing the V atoms incorporated into POMs, but hampered seriously in the presence of slight excess water due to the replaced effect of water for the coordinated HCl and MeCN. Notably, such impediment effect of water was weakened obviously over the  $\text{Q}^+$ -containing POMs due to a hydrophobicity of these POM's. As a result, most of the  $\text{Q}^+$ -containing POMs showed a higher activity for this photo-catalysis reaction in MeCN-HCl- $\text{H}_2\text{O}$  media than the  $\text{H}^+$ -containing counterparts. Isotope tracing test of water-containing heavy oxygen  $^{18}\text{O}$  (97%) in photo-catalysis reaction indicated that the oxygen atoms in water had partly contribution to the formation of cyclohexanol (ca.8.2%) and especially cyclohexanone (ca. 33.3%), which can drastically restrain chlorinated side reactions and thus improve cyclohexanone selectivity. Based on these findings, a free-radical mechanism initiated by the Cl atoms generated in the excited  $\text{POM}\text{-}(\text{V}^{\text{IV}}\text{OHM})^+\text{Cl}^-$  species was proposed.

© 2017 Elsevier B.V. All rights reserved.

## 1. Introduction

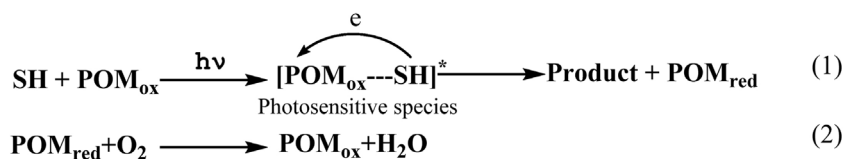
The selective oxygenation of organic compounds by hydrogen peroxide ( $\text{H}_2\text{O}_2$ ) and especially dioxygen ( $\text{O}_2$ ) or air continues to be a very important process due to the large demand for their oxidized products [1]. Among these oxidation reactions, the oxidation of cyclohexane remains in the center of interest of many research groups [1–3] as it provides cyclohexanone and cyclohexanol (KA-oil) as intermediate products in the synthesis of synthetic fibers and fine chemicals [2]. Some efficient catalysis processes have been

developed to achieve the selective oxygenation of cyclohexane or other organic compounds by  $\text{O}_2$  under heating [4–6], UV or visible light illumination [7–14], these catalysis oxidation systems, however, are still more or less disadvantages. For example, the harsh operating conditions (high temperature and pressure) are generally employed in thermal catalysis process, which rarely leads to the chemistry being selective. Most of photo-catalysis processes rely on the excitation of UV light and are still unsatisfactory in transformation efficiency. Consequently, it is highly desirable to develop a simpler and highly-efficient photo-catalysis system for the oxygenation of cyclohexane by  $\text{O}_2$  to KA oil.

In recent decades, polyoxometalate anions (POMs), as an important class of nanosized polynuclear clusters consisting of d-block transition metals and oxygen atoms, have received great attention

\* Corresponding author.

E-mail address: [fzhhnnu@126.com](mailto:fzhhnnu@126.com) (Z. Fu).



**Scheme 1.** A reasonable mechanism for POM-photocatalyzed oxidation of dipolar organic substrates by molecular oxygen.

tion in catalysis due to their variety of applications [15,16]. Among the POMs reported, the two and more highly vanadium atoms-substituted POMs as excellent electron-transfer oxidants, are most often used for the catalytic electron-transfer oxidation of organic substrates [17]. And they can oxidize some substrates by an outer-sphere electron transfer such as  $\alpha$ -terpinene, xanthene, anthracene and others that have higher oxidation potentials ( $>1.3$  V) than themselves (lower than 1.0 V) [18,19]. Marcus theory gives a reasonable explanation how this type of electron transfer oxidations is possible thermodynamically [20,21]. In this theory, the coordination effect between POM and substrate, the dielectric constant, D, of the solvent and, more importantly, the high negative charge nature of POM are considered to play important roles in lowering the free energy ( $\Delta G^0$ ) and promoting the electron transfer oxidation. As a result, the use of POMs as catalysts for photosynthetic processes involving dipolar organic substrates has developed rapidly by the use of molecular oxygen coupled with photochemical activation [22–30]. In these transformations, oxidation of the substrate (SH) is achieved by the formation of photoactive (PA) complex of it with POM compound ( $\text{POM}_{\text{ox}}$ ) and then the light-triggered intramolecular electron transfer from substrate to  $\text{POM}_{\text{ox}}$  [31–33], the reduced POM compound ( $\text{POM}_{\text{red}}$ ) is re-oxidized by dioxygens coupled with the formation of water to complete the catalytic cycle (Scheme 1). The direct oxidation of cyclohexane by most of the excited POMs, however, is very difficult due to its inertness in the formation of PA complex. Interestingly, we recently found that the mixed addenda hetero-polyacids of the formula  $\text{H}_{3+n}\text{PW}_{12-n}\text{V}_n\text{O}_{40}$  and  $\text{H}_{3+n}\text{PMo}_{12-n}\text{V}_n\text{O}_{40}$  (POMs,  $n=1–3$ ), with the participation of concentrated hydrochloric acid (HCl), can efficiently catalyze the oxidation of cyclohexane by  $\text{O}_2$  and  $\text{N}_2\text{O}$  to KA oil under visible light, achieving higher than 18% yield for KA oil [34,35]. Our initial studies indicated that the HCl easily interacts with POM to form a [POM-HCl] PA complex and the latter can be excited by visible light to achieve its intra-molecular electron transfer from  $\text{Cl}^-$  to POM anions, which leads to the generation of  $\text{Cl}^-$  radicals and the reduction of catalysts. The subsequent reactions initiated by the  $\text{Cl}^-$  radicals result in the oxygenation of cyclohexane by  $\text{O}_2$  or  $\text{N}_2\text{O}$  to KA oil and the regeneration of catalysts. And the additive water plays distinctive roles in restraining chlorinated side reactions and improving selectivity for cyclohexanone [34,35]. It is interesting to further study what kind of PA complex is generated exactly in the POM-HCl system and its generation is influenced by what factors, as well as its and water's effects on the POM-catalyzed oxidation of cyclohexane by  $\text{O}_2$  under visible light. Herein, we would report the preliminary research results in these respects.

## 2. Experimental

### 2.1. Reagents and materials

Materials and reagents used in this study were cyclohexane, *n*-hexanol, triphenylphosphine ( $\text{Ph}_3\text{P}$ ), acetonitrile (MeCN), cyanobenzene ( $\text{PhCN}$ ), diethyl ether, 5,5-Dimethylpyrroline-N-oxide (DMPO), 2,2,6,6-Tetramethylpiperidinoxy(TEMPO), acetone, disodium hydrogen phosphate ( $\text{Na}_2\text{HPO}_4 \cdot 12\text{H}_2\text{O}$ ), sodium molybdate ( $\text{Na}_2\text{MoO}_4 \cdot 2\text{H}_2\text{O}$ ), vanadium pentoxide ( $\text{V}_2\text{O}_5$ ), sodium carbonate ( $\text{Na}_2\text{CO}_3$ ), tetrabutyl-ammonium chloride (TBACl),

**Table 1**

The P, Mo and V contents of both V-containing heteropoly anions measured by an ICP method.

Entry	Sample	P (wt%)	V (wt%)	Mo (wt%)	Actual formula
1	$\text{HPMo}_{9}\text{V}_3$	1.980	9.156	53.990	$\text{HPMo}_{8.8}\text{V}_{2.8}$
2	$\text{TBAPMo}_{9}\text{V}_3$	1.307	5.997	35.770	$\text{TBA PMo}_{8.8}\text{V}_{2.8}$

tetramethylammonium chloride (TMACl), cetyl trimethyl ammonium chloride (CTMACl), concentrated hydrochloric acid (HCl), heavy-oxygen water (97 atom%  $^{18}\text{O}$ ), all of which were of analytical grade. Distilled water was used throughout this experiment.

### 2.2. Preparation of V(V)-substituted molybdo-phosphoric acids and their salts

Referring to the method reported in the literature [36], three V(V)-substituted molybdo-phosphoric acids ( $\text{HPMo}_{11}\text{V}_1$ ,  $\text{HPMo}_{10}\text{V}_2$ ,  $\text{HPMo}_9\text{V}_3$ ) were prepared using  $\text{Na}_2\text{HPO}_4 \cdot 12\text{H}_2\text{O}$ ,  $\text{Na}_2\text{MoO}_4 \cdot 2\text{H}_2\text{O}$  and  $\text{V}_2\text{O}_5$  as P, Mo and V sources, respectively. These acids in water were further exchanged with TBA, TMA or CTMA cations under heating condition to yield a precipitate of their quaternary ammonium salts ( $\text{TBAPMo}_{11}\text{V}_1$ ,  $\text{TBAPMo}_{11}\text{V}_2$ ,  $\text{TBAPMo}_9\text{V}_3$ , CTMAPMo<sub>9</sub>V<sub>3</sub>, TMAMo<sub>9</sub>V<sub>3</sub>). The detail operating procedures for the preparation of these POMs can be found in previously published literature [37]. The P, Mo and V contents for both the representative POMs ( $\text{HPMo}_9\text{V}_3$  and  $\text{TBAPMo}_9\text{V}_3$ ) were measured on a Perkin Elmer Optima 5300DV-ICP. As shown in Table 1, the mole ratio of P, Mo and V of both POMs calculated based on the measured data was equal to each other and close to both theoretical one.

### 2.3. Characterization of samples

#### 2.3.1. Spectral characterization

Liquid UV-vis spectra of the POM samples in pure MeCN, MeCN-HCl, MeCN-HCl-H<sub>2</sub>O solution were measured from 200 to 800 nm on UV-2450 spectro-photometer (Shimadzu, Japan) and their transmission FT-IR spectra recorded from 400 to 4000  $\text{cm}^{-1}$  on a Nicolet Nexus 510P FT-IR spectroscopy using a KBr disc. Liquid vanadium-51 NMR spectra of the samples in deuterated acetonitrile ( $\text{CD}_3\text{CN}$ ) were measured on a Bruker Avance III 600 MHz spectrometer with BBFO cryoprobes. The probe temperature was thermostated at  $(25 \pm 0.5)$  °C. The field frequency stabilization was locked to deuterium by placing the sample tubes containing  $\text{CD}_3\text{CN}$ . EPR spectra were measured in 50  $\mu\text{L}$  quartz tubes on a Bruker A300-10/12/S at room temperature. The spectrometer at 9.8 GHz, modulation frequency 100 kHz, modulation amplitude 3G. EPR spectra were simulated using an extended version of the program Bruker WinEPR.

#### 2.3.2. Cyclic voltammetric measurement

Three-electrode configuration and an autolab electro-chemical workstation (Eco Chemie, Holland) were used to measure the cyclic voltammetric (CV) curves of the samples. A glassy carbon electrode (3-mm diameter disk), sheet of platinum foil electrode and KCl-saturated calomel electrode (SCE) were used as the working, counter and reference electrodes, respectively. All the electrochem-

ical experiments were carried out at room temperature (20 °C). All potentials here are reported versus the SCE.

#### 2.4. Procedure of photo-catalytic oxygenation

The visible light-triggered oxidation of cyclohexane by O<sub>2</sub> over various POMs was carried out in a self-assembly photo-reactor equipped with a water-cooled condenser using a 35W tungsten-bromine lamp (light intensity, 535 mW Cm<sup>2</sup>) equipped with an UV light filter as light resource and the concrete operating procedure of photo-catalytic oxygenation could be found in our previously published work [14]. The oxidative products were quantitatively analyzed on an Agilent 6890N gas chromatograph (GC) with a DB-17 polysiloxane capillary column (30 m × 0.32 mm × 0.50 μm) and flame ionization detector (FID) using *n*-hexanol as an internal standard. Notably, with triphenylphosphine to treat the oxidative products for 1 h did not change the ratio of cyclohexanol to cyclohexanone, indicating that cyclohexyl hydroperoxide was absent in the oxidative products [38]. We used high performance liquid chromatography (HPLC method reported by the literature [39]) to not detect out adipic acid in the oxidation products, indicating that a further oxidation of KA oil can be neglected in the present oxidation system.

#### 2.5. Isotope tracing experiment of water-containing heavy oxygen <sup>18</sup>O (H<sub>2</sub><sup>18</sup>O)

In order to ensure the photo-oxidation described above is carried out in the presence of H<sub>2</sub><sup>18</sup>O as far as possible, the fresh MeCN distilled in the presence of calcium hydride, the catalyst TBAPMo<sub>9</sub>V<sub>3</sub> fully dehydrated at 100 °C and the HCl gas dried with concentrated sulfuric acid were used in this study. In typical operating process, 35W tungsten-bromine lamp was immersed in the MeCN (5 mL) solution containing HCl (1.2 mmol), H<sub>2</sub><sup>18</sup>O (0.1 mL), cyclohexane (1 mmol), and TBAPMo<sub>9</sub>V<sub>3</sub> catalyst (0.01 mmol). The reaction mixture was stirred magnetically for 12 h under pure dioxygen atmosphere (1 atm) and sustained visible light irradiation. After photo-reaction, the quantitative analysis of the oxidative products was carried out based on the above described method and the <sup>18</sup>O-containing cyclohexanol and cyclohexanone was detected on GC-MS-QP2010 instrument. (Shimadzu-Corporation, Japan). Mass spectrometer condition was: ionization mode: EI, electron energy 70 eV, interface temperature: 250 °C, ion source temperature: 200 °C, mass scan range: 40 ~ 640 m/z, solvent delay 3.0 min. The flow rate of the carrier gas (helium) was 1.0 mL/min. A split ratio of 1:50 was used for the injection of 0.2 μL of the solutions. The NIST05S.LIB library was used for the mass spectrum analysis.

### 3. Results and discussion

#### 3.1. Characterization of POMs

Some representative POMs were characterized via FT-IR and UV-vis spectra, and the resulting figures are shown in the ESI†. In this, the main results are summarized as follows: i) The four characteristic adsorption peaks in 1100–700 cm<sup>-1</sup>, which are assigned to the Keggin POM anion [40], could be found in the FT-IR patterns of these POMs and they all showed different degrees of red-shift upon the V(V)-containing POMs, which is likely due to the incorporation of hetero-atoms into the primary structure of the Keggin POM anion leading to the reduced structural symmetry [41]. Beside the Keggin structural peaks above-described, the quaternary ammonium cations-containing POMs also displayed the several characteristic peaks at 2959, 2867, 1479 and 1382 cm<sup>-1</sup> assigned to the cations (Fig.S1). ii) UV-vis spectra of these POMs were very similar to each other, consisting of two characteristic adsorption bands at λ

near 220 and 308 nm that are respectively attributed to oxygen to molybdenum charge transfer (LMCT) of the Mo=O<sub>d</sub> and Mo-O<sub>b(c)</sub> bonds in the Keggin structure [42,43]. In comparison with the parent HPMo<sub>12</sub> acid, a blue-shift and a broadening of the Keggin structural band at 308 nm were observed commonly in the UV-vis spectra of all the V(V)-containing POMs, further supporting that the incorporation of hetero-atom into the primary structure of POMs results in reduced structural symmetry [43]. In addition, an absorption band in 400–430 nm could be noticed in the UV-vis spectra of their high concentrations and it was continuously and significantly strengthened and generated a red-shift upon increasing the incorporation of V atoms into POMs (Fig.S2). The addition of HCl to pure MeCN immediately resulted in an obvious raising in the LMCT band of POMs near 220 nm (Fig. S3), which is indicative of a hydrogen bond interactions between the HCl and the Mo=O<sub>d</sub> bond of POMs [44,45]. At the same time, the band in 400–430 nm could shift into the visible by several tens of nanometers and became a broad and strong band in 450–480 nm, this likely implies that POMs can react with HCl to generate some photoactive species, as proposed by Hill and coworkers in investigating the charge-transfer complexes between heteropolytungstic acids and dipolar organic compounds [31].

We previously described in details the CV measurement results of HPMo<sub>12-n</sub>V<sub>n</sub>O<sub>40</sub> (HPAs, n=1-3) in various reaction media with the scanning potential range of -0.4 to 1.2 V and found that the oxidative wave of V<sup>4+</sup> to V<sup>5+</sup> ions in the V(V)-substituted HPAs slightly increased with the incorporated V atoms and was split into two in the presence of HCl [36]. Also, such both phenomena could be noticed in the CV curves of the quaternary ammonium cations-containing POMs (Fig.S4). Notably, the more positive oxidative wave of V<sup>4+</sup> to V<sup>5+</sup> ions near 0.9 V was obviously strengthened with the added HCl amount, but decreased with the added water amount in HPA-HCl system [36], implying that the photoactive species likely corresponds to this more positive wave and its formation is hampered obviously in the presence of water due to replaced effect of water for HCl.

#### 3.2. Photo-catalytic oxidation performance of POMs

**Table 2A** lists the data for the POMs-catalyzed oxygenation of cyclohexane with O<sub>2</sub> in MeCN containing concentrated HCl under visible light irradiation. As shown in **Table 2A**, this photo-oxidation did not occur upon the parent HPMo<sub>12</sub> acid (Entry 1), but could efficiently proceed upon all the V(V)-substituted POMs (Entries 2–9), achieving ca. 24–32% cyclohexane conversion with higher than 91% selectivity for KA oil after 12 h of sustained visible light irradiation, along with the formation of a small amount of chlorocyclohexane (selectivity, 0.9–8.2%). Moreover, the photo-catalytic activity of these V(V)-containing catalysts was gradually improved with increasing the incorporated V atoms, which corresponds well to an improvement in the reoxidation capacity of POMs [46,47]. For example, the conversion over HPMo<sub>12-n</sub>V<sub>n</sub> acids was improved from 24.7 to 29.1% when the V atoms were increased from 1 to 3 (entries 2–4). And these HPMo<sub>12-n</sub>V<sub>n</sub> acids generally showed slightly higher catalysis activity and provided almost identical product distribution compared to the corresponding HPW<sub>12-n</sub>V<sub>n</sub> acids previously reported by us [34]. Notably, most of the quaternary ammonium cations-containing POMs possessed slightly higher activities than the corresponding H<sup>+</sup>-containing ones (entries 6–8 vs 3–4). Entry 10 shows that when the addition of H<sub>2</sub><sup>18</sup>O in the MeCN-TBAPMo<sub>9</sub>V<sub>3</sub>-HCl system could give very similar result to Entry 7.

Some control experiments listed in **Table 2B** show that the oxidation of cyclohexane catalyzed by TBAPMo<sub>9</sub>V<sub>3</sub> was not easy to occur in the absence of HCl and could not happen at all without light illumination (Entries 11–12). Also, the additive HCl itself hardly ini-

**Table 2A**Visible light-driven oxygenation of cyclohexane with O<sub>2</sub> catalyzed by various V(V)-substituted POMs in the presence of concentrated HCl.<sup>a</sup>

Entry	Catalyst	Conv. /%	Selectivity of products <sup>b</sup> (%)		
			Cyclohexanone	Cyclohexanol	Chlorocyclohexane
1	HPMo <sub>12</sub>	0	–	–	–
2	HPMo <sub>11</sub> V <sub>1</sub>	24.7	87.6	11.5	0.9
3	HPMo <sub>10</sub> V <sub>2</sub>	27.8	86.6	12.2	1.2
4	HPMo <sub>9</sub> V <sub>3</sub>	29.1	83.6	12.5	3.8
5	TBAPMo <sub>11</sub> V <sub>1</sub>	24.2	86.3	9.8	3.9
6	TBA PMo <sub>10</sub> V <sub>2</sub>	30.1	83.3	13.2	3.5
7	TBAPMo <sub>9</sub> V <sub>3</sub>	32.2	83.2	12.9	3.9
8	TMAPMo <sub>9</sub> V <sub>3</sub>	30.2	79.2	14.0	6.8
9	CTMAPMo <sub>9</sub> V <sub>3</sub>	28.9	78.4	13.4	8.2
10 <sup>c</sup>	TBAPMo <sub>9</sub> V <sub>3</sub>	32.2	84.7	12.1	3.2

<sup>a</sup> Cyclohexane, 1.0 mmol, catalyst, 0.01 mmol, MeCN, 4.9 mL, concentrated HCl, 0.1 mL, O<sub>2</sub>, 1 atm, temperature, 36–38 °C, time, 12 h, using 35 W of tungsten-bromine lamp.<sup>b</sup> Product selectivity = the content of this product/Σ content (mmol) of each product × 100%.<sup>c</sup> Adding 0.1 mL of H<sub>2</sub><sup>18</sup>O in the reaction system containing 1.2 mmol of dry HCl.**Table 2B**The data obtained from the TBAPMo<sub>9</sub>V<sub>3</sub>-photocatalyzed oxygenation of cyclohexane under different conditions.<sup>a</sup>

Entry <sup>a</sup>	Additive/Gas	Solvent	Conv. /%	Selectivity of products (%)		
				Cyclohexanone	Cyclohexanol	Chlorocyclohexane
11 <sup>b</sup>	–/O <sub>2</sub>	MeCN	2.9	57.5	43.1	–
12 <sup>c</sup>	HCl/O <sub>2</sub>	MeCN	0	–	–	–
13 <sup>d</sup>	HCl/O <sub>2</sub>	MeCN	1.2	71.3	28.7	–
14	HNO <sub>3</sub> /O <sub>2</sub>	MeCN	0.29	62.1	37.9	–
15	H <sub>2</sub> SO <sub>4</sub> /O <sub>2</sub>	MeCN	0.54	14.8	85.2	–
16	HBr/O <sub>2</sub>	MeCN	0.10	100	–	–
17	HCl/Air	MeCN	24.7	75.6	17.4	7.0
18 <sup>e</sup>	HCl/N <sub>2</sub>	MeCN	14.2	76.1	13.9	10.0
19 <sup>e</sup>	Dry HCl/N <sub>2</sub>	MeCN	4.7	36.7	18.9	44.4
20	HCl/O <sub>2</sub>	Acetone	11.8	78.0	17.7	4.3
21	HCl/O <sub>2</sub>	PhCN	18.8	53.0	45.6	1.4
22 <sup>f</sup>	HCl + DMPO/O <sub>2</sub>	MeCN	3.2	79.1	17.8	3.1

<sup>a</sup> Cyclohexane, 1.0 mmol, catalyst, 0.01 mmol, solvent, 4.9 mL, acidic additive, 1.2 mmol, water, 0.1 mL, 1 atm, temperature, 36–38 °C, time, 12 h, using 35 W of tungsten-bromine lamp.<sup>b</sup> Without acidic additive.<sup>c</sup> Under heating (35 °C) but without light illumination.<sup>d</sup> Without catalyst.<sup>e</sup> The time of using nitrogen to run out the air inside reactor, 20 min.<sup>f</sup> Adding DMPO(0.1 mmol), reaction time, 5 h.

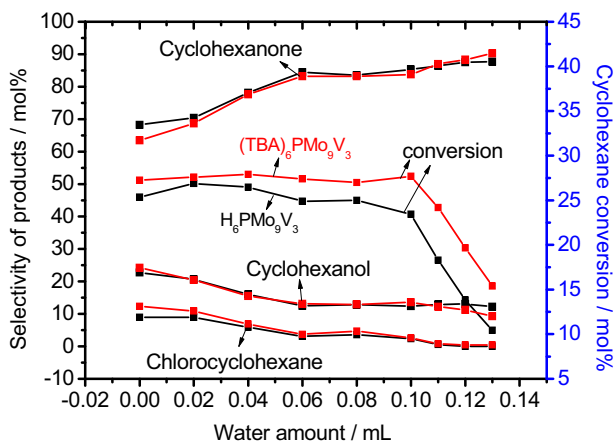
tiated such photo- oxidation in the absence of catalyst (Entry 13). In addition, the other acidic additives such as sulfuric acid (H<sub>2</sub>SO<sub>4</sub>), nitric acid (HNO<sub>3</sub>) and hydrobromic acid (HBr) were invalid to promote this photo-catalysis reaction (Entries 14–16). Notably, the present photo-catalysis reaction could proceed efficiently under air although its efficiency was lower than that obtained under pure O<sub>2</sub> (Entries 17 vs 7). Also, such photo- catalysis reaction could occur under inert N<sub>2</sub> and concentrated HCl, achieving ca. 14.1% conversion with slightly high chlorination (entry 18). But it's efficiency drastically declined and serious chlorination by-reaction was observed under inert N<sub>2</sub> and anhydrous HCl gas (entry 19). Entries 20 and 21 show that acetone and cyanobenzene (PhCN) could be used as efficient reaction media, but the conversion in such two solvents was by much lower than that in MeCN. Entries 22 show that the addition of DMPO could drastically hamper the present photo-catalysis reaction.

It is concluded from the results in Tables 2A and 2B that i) the direct photo-oxidation of cyclohexane by O<sub>2</sub> is very difficult even if the V(V)-substituted POMs with a stronger oxidation capacity were used as catalysts, this is likely because a photoactive complex of POM with cyclohexane is not easy to be generated due to a known inertness of the substrate. ii) Only the HCl is an efficient acid additive for the V(V)-substituted POM-catalyzed cyclohexane oxidation in MeCN under visible light illumination, this may be because it easily reacts with the V(V)-substituted POMs to form a highly photoactive (PA) species. iii) The formation of PA species

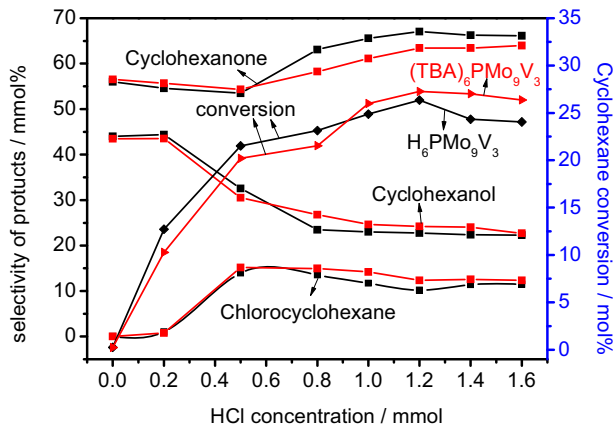
is likely influenced by the incorporated V(V) atom number and the cations of POMs. iv) The additive water likely participates the oxidation of cyclohexane by some way, as supported by the experiment in entry 18. v) The present photo-oxidation should have a characteristics of free radical initiation and is likely initiated the Cl free radicals generated by visible light excitation of the PA species, as supported by the results in entries 19 and 22.

### 3.3. A detail comparison of catalysis activity of HPMo<sub>9</sub>V<sub>3</sub> and TBAPMo<sub>9</sub>V<sub>3</sub>

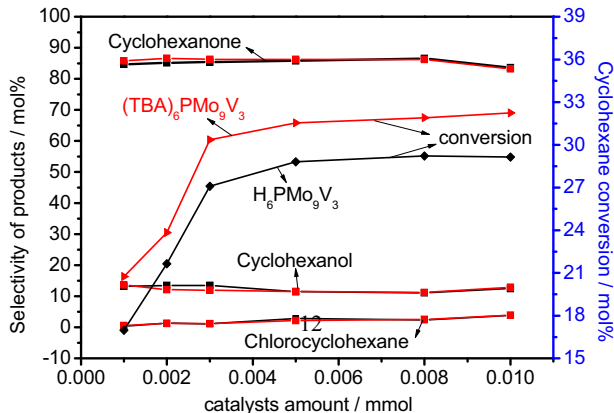
In the following experiments, the photo-catalytic activities of HPMo<sub>9</sub>V<sub>3</sub> and TBAPMo<sub>9</sub>V<sub>3</sub> for the oxidation of cyclohexane by O<sub>2</sub> in MeCN under visible light irradiation were further checked by varying the amount of HCl, water or catalyst, as well as irradiation time and the results are shown in Figs. 1–4. Fig. 1 shows that when the amount of water in MeCN-containing 1.2 mmol HCl did not exceed 0.04 mL for HPMo<sub>9</sub>V<sub>3</sub> and 0.1 mL for TBAPMo<sub>9</sub>V<sub>3</sub>, cyclohexane conversion over both the POMs was almost unchanged with the amount and could maintain about 26.5 and 27.6%, respectively. And cyclohexanone selectivity was significantly improved with the amount and achieved about 85% in the presence of 0.1 mL water, along with a decrease of cyclohexanol and chlorocyclohexane. When the added water exceeded the amount above-mentioned, the conversion over both POMs continuously decreased with the amount and the selectivity for cyclohexanone was further



**Fig. 1.** Effect of water amount on the POM (0.003 mmol)-photocatalyzed cyclohexane (1 mmol) oxidation by O<sub>2</sub> in MeCN (5.0 mL) with dry HCl (1.2 mmol) under visible light irradiation (8 h).

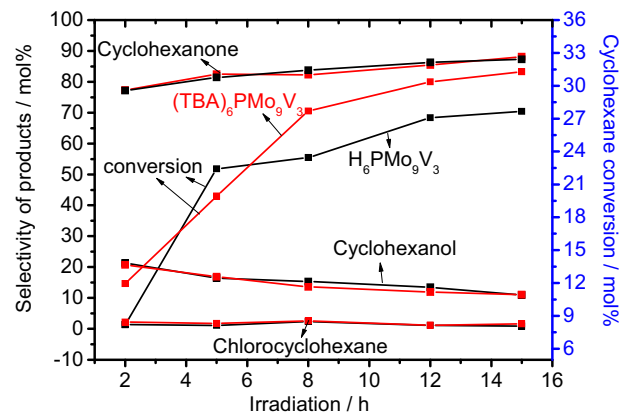


**Fig. 2.** Effect of HCl amount on the POM (0.003 mmol)-photocatalyzed oxidation of cyclohexane (1 mmol) by O<sub>2</sub> in MeCN (5.0 mL) under visible light irradiation (8 h).



**Fig. 3.** Effect of catalyst amount on the photo-catalysis oxidation of cyclohexane (1 mmol) by O<sub>2</sub> in MeCN (4.9 mL) with HCl (12 M, 0.1 mL) under visible light irradiation (12 h).

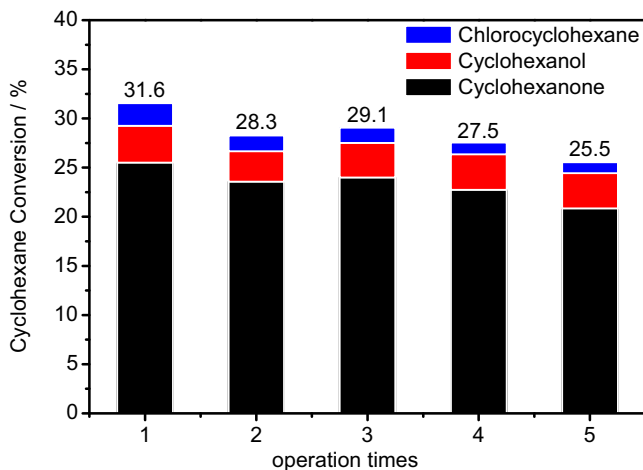
improved to near 90%. And the CTMAPMo<sub>9</sub>V<sub>3</sub> possessed slightly stronger water resistance than TBAPMo<sub>9</sub>V<sub>3</sub> and its catalytic activity was nearly unchanged when water amount was enhanced to 0.11 mL (Fig.S5). These findings illustrate that the additive water, as previously reported by us [34,35], can significantly improve cyclohexanone selectivity, but it hampers this photo-catalysis oxidation in the case of its slight excess amount. Notably, such interfer-



**Fig. 4.** Effect of irradiation time on the POMs (0.003 mmol)-photocatalyzed cyclohexane (1 mmol) oxidation by O<sub>2</sub> in MeCN (4.9 mL) with HCl (12 M, 0.1 mL) under visible light irradiation.

ence effect is weakened evidently over TBAPMo<sub>9</sub>V<sub>3</sub>, especially CTMAPMo<sub>9</sub>V<sub>3</sub> owing to the hydrophobicity of such two POMs. Fig. 2 shows that when the amount of HCl in MeCN was between 0.2 and 1.2 mmol, cyclohexane conversion continuously increased with the amount and achieved its maximum at 1.2 mmol (26.4% for HPMo<sub>9</sub>V<sub>3</sub> and 27.3% for TBAPMo<sub>9</sub>V<sub>3</sub>). After that, it gradually decreased over HPMo<sub>9</sub>V<sub>3</sub> and hardly varied over TBAPMo<sub>9</sub>V<sub>3</sub> with further increasing HCl amount. The activity of TBAPMo<sub>9</sub>V<sub>3</sub> was slightly inferior to that of HPMo<sub>9</sub>V<sub>3</sub> under low HCl amount (0.2–0.9 mmol), but the opposite result was obtained when HCl amount was higher than 0.9 mmol. Fig. 3 demonstrates that when the amount of catalyst was enhanced from 0.001 to 0.003 mmol, cyclohexane conversion continuously increased from 17.0 to 27.1% over HPMo<sub>9</sub>V<sub>3</sub> and 20.7–30.4% over TBAPMo<sub>9</sub>V<sub>3</sub>. After that, the conversion slightly increased over HPMo<sub>9</sub>V<sub>3</sub> and was almost unchanged over TBAPMo<sub>9</sub>V<sub>3</sub> with a further increasing POM to 0.01 mmol. Fig. 4 shows that when the time was prolonged from 2 to 12 h, the conversion of cyclohexane was continuously and significantly improved from 8.2 to 27.1% over HPMo<sub>9</sub>V<sub>3</sub> and 11.9–30.4% over TBAPMo<sub>9</sub>V<sub>3</sub>. After that, it slightly increased with the further prolonging time to 15 h. On the whole, cyclohexanone selectivity continuously and slowly increased with increasing irradiation time and the amount of POM or especially HCl, companying a decrease in cyclohexanol selectivity. The formation of chlorocyclohexane was influenced slightly by such three variables and the distribution of products over both the POMs was hardly different.

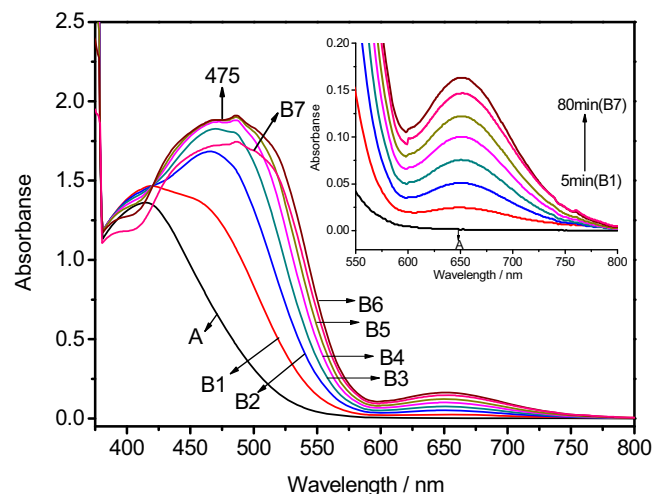
Finally, the reuse of TBAPMo<sub>9</sub>V<sub>3</sub> in the concentrated HCl-assisted oxygenation of cyclohexane by O<sub>2</sub> in MeCN under visible light illumination was checked under the same conditions with the entry 7 in Table 2A. After the first reaction was carried out and the reaction products were analyzed by GC, the resulting yellow-green solution was evaporated to dry with the rotary evaporator to precipitate catalyst, the obtained catalyst was dissolved with pure MeCN and the resulting solution without reactants and products confirmed by GC analysis was subjected to the next photo-reaction under same conditions. As shown in Fig. 5, the conversion of cyclohexane decreased gradually with recycling times and its decreased degree each recycling run was about 2% until the fifth operating. After that, the conversion over the recovered catalyst was remarkably reduced to 15.2% in the sixth operating. By the way, the distribution of products each recycling run was basically equal to each other. This indicates that the recovered catalyst has a good stability and can maintain higher than 25% conversion during five recycles of operation.



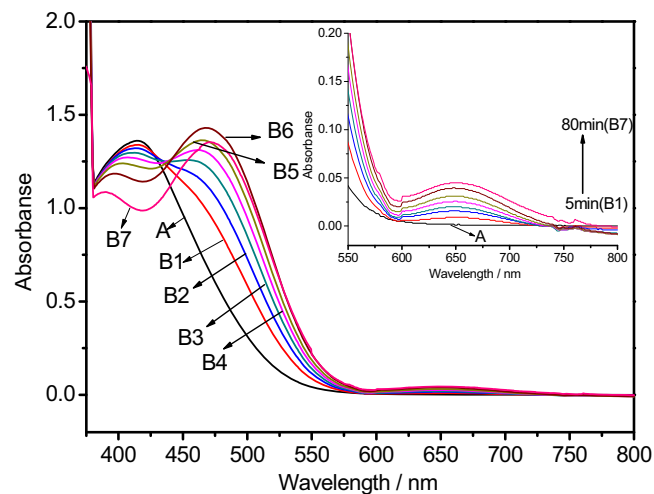
**Fig. 5.** The catalyst's repeatability in photo-catalysis oxygenation of cyclohexane with  $O_2$  promoted by concentrated HCl.

#### 3.4. Study on the photoactive species generated in POM-HCl system

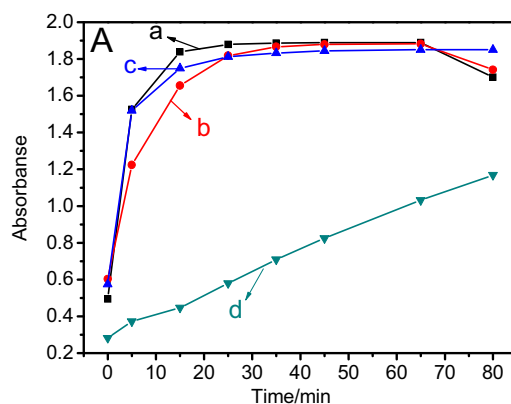
In order to explore what kind of photoactive (PA) species is generated in POM-HCl system and its formation is influenced by what factors, we measured UV-vis spectral changes (in 400–800 nm) of several typical POMs in MeCN-HCl media and some very important spectral changes in 400–800 nm are summarized as follows using TBAPMo<sub>9</sub>V<sub>3</sub> as an example (Fig. 6): i) An adsorption bands near 415 nm, assignable to the charge transfer transition from oxygen to the coordinated Mo or V atoms [48], could be found in its spectrum (curve A in Fig. 6). When HCl gas was introduced to the A solution, such band immediately rose, then gradually decayed and took place blue-shift with the interaction time of HCl and became finally shifted to lower than 400 nm at 80 min (curves B1–B7). ii) At the same time, the absorption curve in 450–500 nm rapidly drove up in the presence of HCl, and was gradually strengthened and gave rise to red-shift on further increasing the interaction time and achieved a maximum and became a broad and strong band with  $\lambda_{\text{max}} = 475$  nm at 45 min. However, such spectral change did not occur in the HPMo<sub>12</sub>-HCl system (Fig. S6). This implies that the only oxo-vanadium(V) species of TBAPMo<sub>9</sub>V<sub>3</sub> can capture HCl to form an D-A complex, and then the latter is gradually converted to form some PA species. iii) The absorbance in 600–800 nm, which is attributed to an intervalence charge transfer of the reduced POMs [44,49], synchronously increased with the band at 475 nm and achieved a maximum at 65 min. After that, it slightly fell



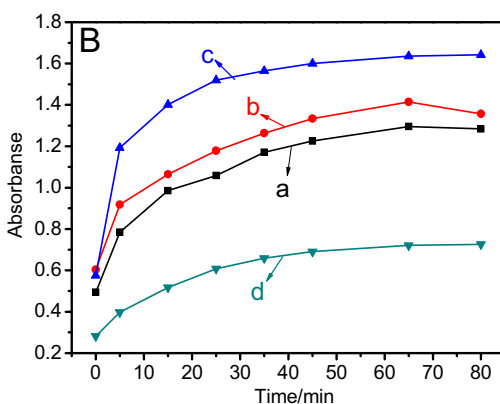
**Fig. 6.** UV-vis spectra (200–800 nm) of TBAPMo<sub>9</sub>V<sub>3</sub> (0.003 mmol) in MeCN (5.0 mL) with dry HCl (1.2 mmol). **A:** the system in a pure MeCN; **B1–B7:** After adding HCl to the system **A** for 5, 15, 25, 35, 45, 65 and 80 min. Inset is its amplification part in 550–800 nm.



**Fig. 7.** UV-vis spectra (200–800 nm) of TBAPMo<sub>9</sub>V<sub>3</sub> (0.003 mmol) in MeCN (4.95 mL) with dry HCl (1.2 mmol) and  $H_2O$  (0.05 mL). **A:** the system in a pure MeCN; **B1–B7:** After adding HCl and  $H_2O$  to the system **A** for 5, 15, 25, 35, 45, 65 and 80 min. Inset is its amplification part in 550–800 nm.



**Fig. 8.** The interaction time-dependence absorbance at 475 nm in the absence (**A**) or presence (**B**) of water. (**a**): HPMo<sub>9</sub>V<sub>3</sub>; (**b**): TBAPMo<sub>9</sub>V<sub>3</sub>; (**c**): CTMAPMo<sub>9</sub>V<sub>3</sub>; (**d**): HPMo<sub>12</sub>V.



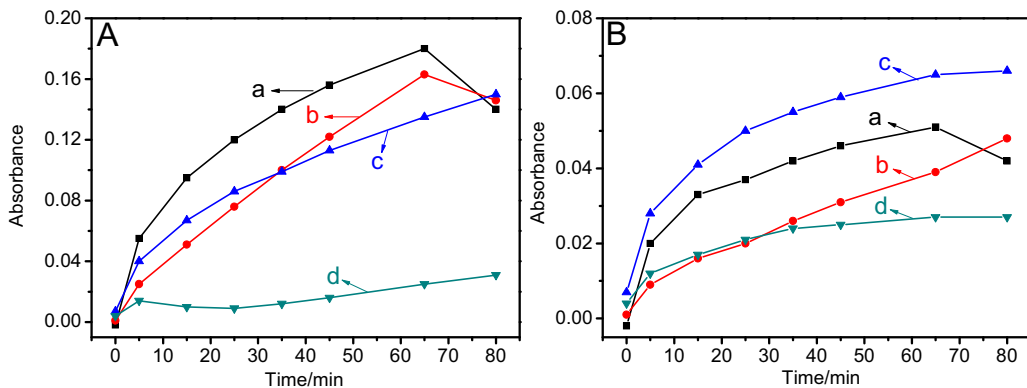


**Fig. 9.** The interaction time-dependence absorbance at 650 nm in the absence (A) or presence (B) of water. (a): HPMo<sub>9</sub>V<sub>3</sub>; (b): TBAPMo<sub>9</sub>V<sub>3</sub>; (c): CTMAPMo<sub>9</sub>V<sub>3</sub>; (d): HPMo<sub>12</sub>V.

(see inset in Fig. 6). This indicates that the reduction of such PA species to its V(IV) species can also occur under daylight illumination. Fig. 7 presents the exerted effect of water on the spectral changes described above. In that, the addition of water (0.05 mL) could obviously slow down the decay rate of the LMCT band near 408 nm, thereby decrease the formation rate of both bands at 450–500 and 600–800 nm, which is likely due to an interference effect of water on the formation of such PA species. The spectral changes above-described could be noticed in the UV-vis spectra of HPMo<sub>9</sub>V<sub>3</sub>, CTMAPMo<sub>9</sub>V<sub>3</sub> and HPMo<sub>11</sub>V in MeCN-HCl or MeCN-HCl-H<sub>2</sub>O media (Figs.S7–12).

In order to further compare the differences among the spectral changes of these POMs under HCl interaction, the interaction time-dependence absorbances at 475 and 650 nm are defined as the formation rate of such PA species and its conversion rate to the V(IV) species, respectively. The following results can be summarized from Figs. 8 and 9: i) The three V atoms-substituted POMs possessed a much faster rate for the formation of PA species than the one V atom-containing HPMo<sub>11</sub>V<sub>1</sub> in MeCN-HCl media whether water was absent or present (Fig. 8A and B), indicating that the formation rate of PA species is proportional to the V atoms incorporated into POM. ii) The formation rate of such PA species over HPMo<sub>9</sub>V<sub>3</sub> in pure MeCN was slightly faster than that over CTMAPMo<sub>9</sub>V<sub>3</sub> or especially TBAPMo<sub>9</sub>V<sub>3</sub> in the former period but such difference in rate over three POMs was nearly neglected in the latter period (Fig. 8A); In the presence of water, the formation rate for the PA species followed an increasing sequence of CTMAPMo<sub>9</sub>V<sub>3</sub> > TBAPMo<sub>9</sub>V<sub>3</sub> > HPMo<sub>9</sub>V<sub>3</sub> (Fig. 8B), further supporting that TBAPMo<sub>9</sub>V<sub>3</sub> and especially CTMAPMo<sub>9</sub>V<sub>3</sub> have outstanding water resistance and can weaken significantly the interference effect of water on the formation of PA species, which is consistent with the above reaction results. iii) The HPMo<sub>11</sub>V<sub>1</sub> always provided a lower rate for the generation of V(IV) species than the three V atoms-substituted POMs (Fig. 9A and B), which should be due to its low V substitution. The generation rate of V(IV) species over HPMo<sub>9</sub>V<sub>3</sub> was higher than that over CTMAPMo<sub>9</sub>V<sub>3</sub> in the absence of water (curves a vs c in Fig. 9A), but a contrary result could be observed in the presence of water (curves a vs c in Fig. 9B), which corresponded basically to the formation rate of PA species. However, such rate over TBAPMo<sub>9</sub>V<sub>3</sub> was still slower than that over HPMo<sub>9</sub>V<sub>3</sub> even if water was present (curves b vs a in Fig. 9B). In order to explore the reason that leads to this difference, we used UV-vis spectra to monitor the oxidation of triphenylphosphine by the PA species. As shown in Fig. 10, such band attributable to the PA species nearly disappeared after the addition of triphenylphosphine for 15 min owing to the redox reaction [50]. Notably, this band over TBAPMo<sub>9</sub>V<sub>3</sub> could be recovered most after 3 h, but its recovery was unsatisfactory over CTMAPMo<sub>9</sub>V<sub>3</sub> and especially

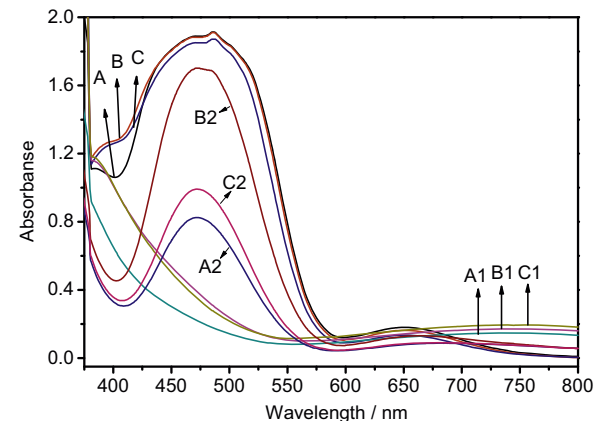


**Fig. 10.** UV-vis spectral changes of photoactive species over HPMo<sub>9</sub>V<sub>3</sub> (0.003 mmol), A) TBAPMo<sub>9</sub>V<sub>3</sub> (B) and CTMAPMo<sub>9</sub>V<sub>3</sub> (C) in MeCN (5.0 mL)-HCl (1.2 mmol) media before and after treatment with Ph<sub>3</sub>P (0.005 mmol). (A, B, C): After 65 min of adding dry HCl to the POM-MeCN system; (A1, B1, C1): After 15 min of adding Ph<sub>3</sub>P to the system A, B or C; (A2, B2, C2): After 3 h of adding Ph<sub>3</sub>P to the system A, B or C.

HPMo<sub>9</sub>V<sub>3</sub>. This indicates that the TBAPMo<sub>9</sub>V<sub>3</sub> has an outstanding capacity in catalytic recycling between its photoactive V(V) and V(IV) species, which can lead to lowered cumulant of the V(IV) species and improved its photocatalysis efficiency. These spectral characterization results are well consistent with the above reaction ones.

The following <sup>1</sup>V NMR and supplementary UV-vis spectra were further used to study a character of the PA species above-described. As shown in Fig. 11, HPMo<sub>9</sub>V<sub>3</sub> with a good solubility in pure deuterated acetonitrile (CD<sub>3</sub>CN), displayed at least six <sup>51</sup>V NMR peaks with chemical shifts of -557, -561, -564, -565, -573 and -583 ppm (Curve a), which can be indicative of the co-existence of multiple positional  $\alpha$  isomers in two or more V atoms-substituted POMs [51]. After treatment with concentrated HCl, these <sup>51</sup>V resonances were shifted to downfield and reduced to four peaks with chemical shifts of -550, -552, -554 and -562 ppm (Curve b). And Pettersson and coworkers previously reported that the <sup>51</sup>V resonances for HPMo<sub>11</sub>V<sub>2</sub> in an acidic aqueous solution appeared in much lower field (-520 to -540 ppm) [52]. We propose from these facts that this shift phenomenon perhaps originates from the exerted protonation and hydration effects of concentrated HCl on these  $\alpha$  isomers and such protonation likely occurs upon the POM's V-O<sub>c</sub>-Mo and V-O<sub>c</sub>-V sites with the most basic of edge-sharing oxygens [52]. Notably, the <sup>51</sup>V NMR signal at -550 ppm was the strongest among these <sup>51</sup>V NMR resonances, and only its intensity further increased with prolonging the interaction time of HCl (Curves c-d vs b). At the present, we do not know that such <sup>51</sup>V NMR peak at

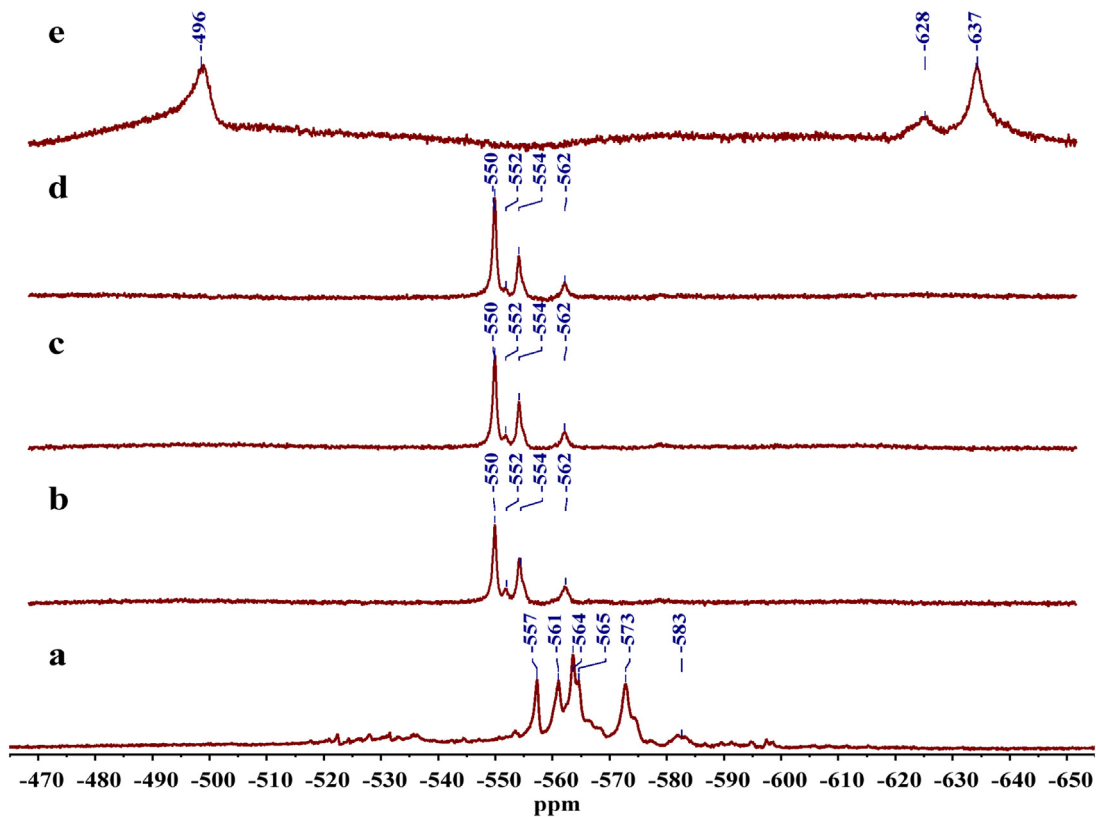


**Fig. 11.**  $^{51}\text{V}$  NMR of a solution of  $\text{HPMo}_9\text{V}_3$  (10 mM) in  $\text{CD}_3\text{CN}$ . (a) the system in a pure  $\text{CD}_3\text{CN}$ . After adding  $\text{HCl}$  (0.72 mM) to system a for (b) 180 min, (c) 240 min, (d) 300 min. (e) The system of  $\text{NaVO}_3$ - $\text{HNO}_3$ - $\text{H}_2\text{O}_2$  in  $\text{CD}_3\text{CN}$ .

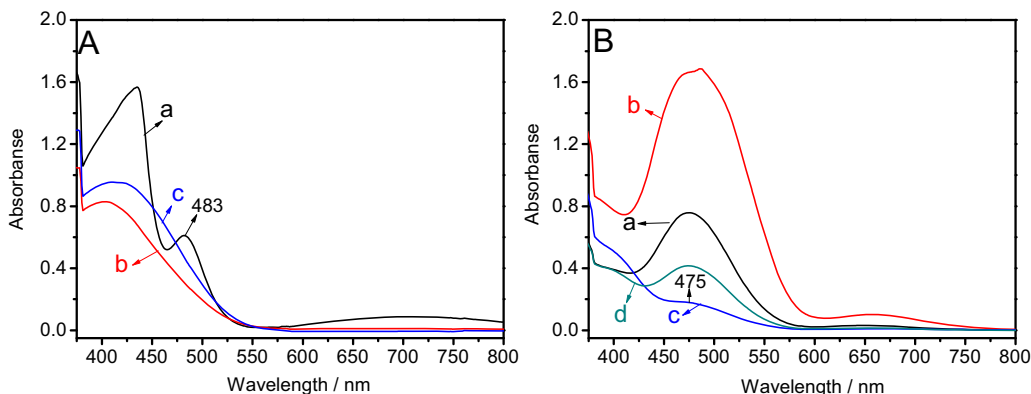


**Fig. 12.** UV-vis spectra (200–800 nm) of  $\text{TBAPMo}_9\text{V}_3$  (0.003 mmol) in  $\text{MeCN}$  (4.90 mL) –containing various acidic additives (A) or various solvents-containing concentrated  $\text{HCl}$  (0.1 mL, 12 M, B). Diagram A: After adding a)  $\text{HBr}$  (0.1 mL, 7.4 M), b)  $\text{H}_2\text{SO}_4$  (1.2 mmol), or c)  $\text{HNO}_3$  (0.1 mL, 16 M) for 100 min; Diagram B: a) in  $\text{MeCN}$  (4.90 mL) for 420 min, b) in  $\text{PhCN}$  (4.90 mL) for 420 min, c) in acetone (4.90 mL) for 420 min, d) After adding 0.01 mL water to the system a for 420 min.

–550 ppm should be specifically assigned to which protonated  $\alpha$  isomer, but it should be relative to the PA species. And the possibility that it is attributable to the oxo-monoperoxo-vanadium(V) species ( $\text{V}^{\text{V}}\text{O}(\text{O}_2)^+$ ) with a characteristic band of 475 nm reported Okuhara [53a] and Waidmann [53b], can be excluded based on the following facts: A  $^{51}\text{V}$  NMR spectrum for the  $\text{NaVO}_3$ - $\text{HNO}_3$ - $\text{H}_2\text{O}_2$  system in  $\text{CD}_3\text{CN}$  exhibited three  $^{51}\text{V}$  NMR peaks (curve e), in which one peak at –496 ppm should be assigned to the  $\text{V}^{\text{V}}\text{O}(\text{O}_2)^+$  species and another two peaks at –628 and –637 ppm are attributable to the oxo-diperoxo-vanadium(V) ( $\text{VO}(\text{O}_2)_2^+$ ) species [54]. Such three  $^{51}\text{V}$  NMR peaks, however, were absent in a  $^{51}\text{V}$  NMR spectrum of the  $\text{HPMo}_9\text{V}_3$ - $\text{HCl}$  system. The supplementary UV-vis spectra can provide some important information for further understanding such PA species. As shown in Fig. 12A, when other acid such as

$\text{HBr}$ ,  $\text{H}_2\text{SO}_4$  or  $\text{HNO}_3$  instead of  $\text{HCl}$  was used as an acidic additive, such PA species was also generated in  $\text{HBr}$  and its characteristic absorption band red-shifted to 483 nm, along with the stronger absorbance in 600–800 nm (curve a), but such spectral changes did not occur in the presence of  $\text{H}_2\text{SO}_4$  or  $\text{HNO}_3$  (curve b and c). This implies that such PA species should be relative to the halide anions and its characteristic band is likely assigned to charge transfer (LMCT) of halide anions to the protonated  $\text{V}^{\text{V}}\text{-O}_c\text{-V}^{\text{V}}$  or  $\text{V}^{\text{V}}\text{-O}_c\text{-Mo}^{\text{VI}}$  sites. And the  $\text{Br}^-$  anion takes place such charge transfer more easily than the  $\text{Cl}^-$  one due to its good electron-donating ability, resulting in generating a strong and red-shifted LMCT. But such  $\text{Br}^-$ -containing PA species, as shown in the entry 16 of Table 2B, was invalid to the present photo-catalysis oxidation, this is likely because the  $\text{Br}$  atom formed by light-driven such PA species, as a

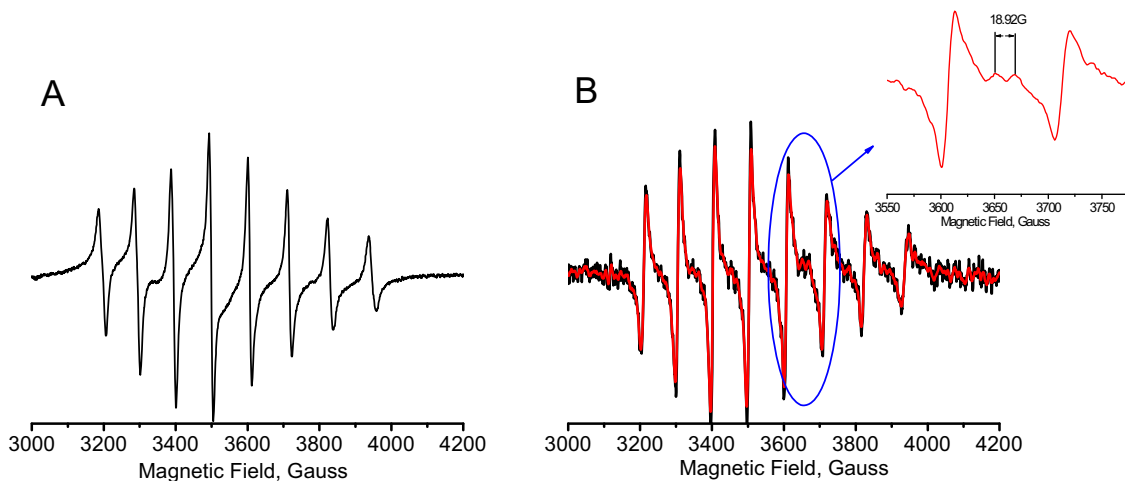


**Fig. 13.** Experimental EPR spectra of  $\text{TBAPMo}_9\text{V}_3\text{O}_{40}$  (0.1 mmol), dry  $\text{HCl}$  gas (1.2 mmol) dissolved in  $\text{MeCN}$  (5 mL) under  $\text{N}_2$  and visible light illumination 2.5 h in the absence (Part A) and presence (Part B) of DMPO (2 mmol). The red curve is a smoothing spectrum of the curve B, and the inset is its amplification part in 3600–3700 G. (For interpretation of the references to colour in this figure legend, the reader is referred to the web version of this article.)

low reactive radical [55], can not initiate the oxidation of cyclohexane by  $\text{O}_2$ . Fig. 12B shows that the solvent exerted an obvious effect on the LMCT band attributable to the PA species generated in the  $\text{TBAPMo}_9\text{V}_3$ – $\text{HCl}$  system, as shown in Fig. 12B, such LMCT band in  $\text{PhCN}$  became very strong and gave a slight blue-shift (curve **a**) compared to that in  $\text{MeCN}$  (curve **b**). But it in acetone was very weak and appeared at 475 nm (curve **c**). Notably, such LMCT band in  $\text{MeCN}$  drastically declined after adding 0.01 mL water (curve **d**). The spectral change of PA species in these solvents, as reported previously in the metal chloride ( $\text{CuCl}_2$ ,  $\text{FeCl}_3$  or  $\text{VOCl}_3$ ) photo-catalysis system [14a], likely originates from the weak coordination effect of solvent molecules with the PA species [56]. Such coordination effect of  $\text{MeCN}$ ,  $\text{PhCN}$  or acetone as electron-accepting molecule usually leads to the LMCT band being red-shifted to the visible light region. On the contrary,  $\text{H}_2\text{O}$  as electron-donating molecule results in blue-shift of the LMCT band to UV light region [57]. And the reason that adding slightly excess of water results in an obvious decrease of the LMCT band is likely due to the substitution of water to the  $\text{MeCN}$  molecule coordinated to the PA species, namely the hydration effect above-described in the  $^{51}\text{V}$  NMR spectra.

Electron paramagnetic resonance (EPR) was used to measure the photo-triggered redox products of the PA species. As shown in the curve **a** of Fig. 13A, after a  $\text{MeCN}$  solution containing  $\text{TBAPMo}_9\text{V}_3$  and dry  $\text{HCl}$  was illuminated by visible light for 2.5 h under  $\text{N}_2$ , its EPR spectrum yielded a 8-line spectrum attributable to a  $\text{V}^{\text{IV}}$  ( $I = 7/2$ ) containing polyoxometalate [61], demonstrating that a reduction of the  $\text{V}^{\text{V}}$  to  $\text{V}^{\text{IV}}$  of PA species indeed occurs in the present photo-reaction. If the above light illumination reaction was carried out in the presence of DMPO, its EPR spectrum still exhibited a 8-line spectrum of  $\text{V}^{\text{IV}}$  above described and two very weak EPR signals with  $A_N = 18.92\text{G}$  in 3600–3700G (Fig. 13B). Such two EPR signals, which possess a similar  $A_N$  value to the EPR signals of DMPO-captured  $\text{Cl}$  free radical in benzene reported by Buettner ( $A_N = 19.67\text{G}$ ), are suspected to originate from the DMPO- $\text{Cl}$  radical adduct [62]. In order to explore the reason to yield such very weak EPR signals, we used a simulated N-O free radical TEMPO to check whether it reacts the present catalysis system. The results showed that TEMPO can be rapidly oxidized by catalyst in the presence of  $\text{HCl}$ , leading to the extermination of its EPR signals (Fig.S13). Therefore, the generation and then extermination of DMPO- $\text{Cl}$  radical adduct may simultaneously occur in the present trapping reaction, which will make it difficult to produce the convincing EPR signals attributable to such radical adduct.

Finally, an isotope tracing test of heavy oxygen water ( $\text{H}_2^{18}\text{O}$ ) for the present photo-catalytic oxidation was used to investigate the regulated effect of water on photo-oxidation products. Fig. 14 is the mass spectra of cyclohexanol and cyclohexanone obtained in the presence of  $\text{H}_2^{18}\text{O}$ . Three  $^{16}\text{O}$ -containing fragment peaks with mass to charge ratios ( $m/z$ ) of 44, 57 and 72 appeared in a mass spectrum of cyclohexanol (Fig. 14A). One  $^{18}\text{O}$ -containing fragment peak with  $m/z$  ratio of 59 was also observed except the above three peaks and an intensity ratio of it with the corresponding peak at  $m/z$  of 57 was 9: 100 (the content of  $^{18}\text{O}$ -containing component estimated was ca. 8.2%). Fig. 14B shows that a mass spectrum of cyclohexanone exhibited four  $^{16}\text{O}$ -containing fragment peaks with  $m/z$  ratios of 55, 70, 83 and 98, in addition, the four corresponding  $^{18}\text{O}$ -containing fragment peaks with  $m/z$  ratios of 57, 72, 85 and 100 were clearly observed in its mass spectrum and an average intensity ratio of them with the  $^{16}\text{O}$ -containing fragment peaks was about 1:2 (the content of  $^{18}\text{O}$ -containing component estimated was ca. 33.3%). Notably, these  $^{18}\text{O}$ -containing fragment peaks described above were not found in the catalysis system containing concentrated  $\text{HCl}$  or only  $\text{H}_2^{18}\text{O}$  (Figs.S14–15). The isotope tracing test forcefully indicate that the O atoms in water can participate the oxidation of cyclohexane under the present reaction conditions and mainly contributes to the formation of cyclohexanone, as supported by the above reaction results.

### 3.5. Photo-catalytic mechanism

Based on the results presented here, we would carry out a reasonable revision for our previously reported photo-catalytic mechanism [35]. As shown in Scheme 2, firstly, the solvated POM can capture  $\text{HCl}$  to generate a PA species ( $\text{POM}-[\text{V}^{\text{V}}\text{OHM}]^+\text{Cl}^-$ ) via protonation of its  $\text{V}^{\text{V}}-\text{O}_c-\text{M}$  ( $\text{M}$  for  $\text{V}^{\text{V}}$  or  $\text{Mo}^{\text{VI}}$ ) sites. It is most likely, such PA species can be excited by visible light to achieve an intramolecular electron transfer from its  $\text{Cl}^-$  anion to the  $\text{V}^{\text{V}}$  center of the protonated  $[\text{V}^{\text{V}}\text{OHM}]^+$  sites, which can lead to the formation of the reduced POM species and  $\text{Cl}$  atom ( $\text{Cl}\cdot$ ). Such light-driven electronic transfer (ET) oxidation, which was previously reported in the  $\text{FeCl}_3$  [14a,58] and  $\text{CuCl}_2$  photo-catalysis systems [59], is supported by the following facts: i) The formation of the  $\text{V}^{\text{IV}}$ -containing POM in the present photoreaction has been confirmed by EPR spectrum. ii) The formation of the oxidized product  $\text{Cl}$  free radical lacks the convincing EPR proof at present, but it is supported forcefully by the following facts: The chlorinated by-reaction always exists in the present reaction system and becomes more serious under

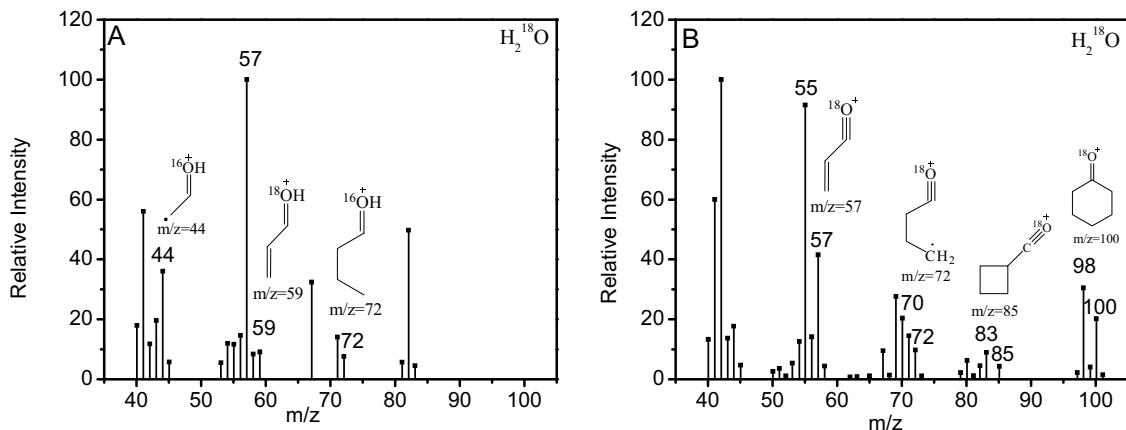
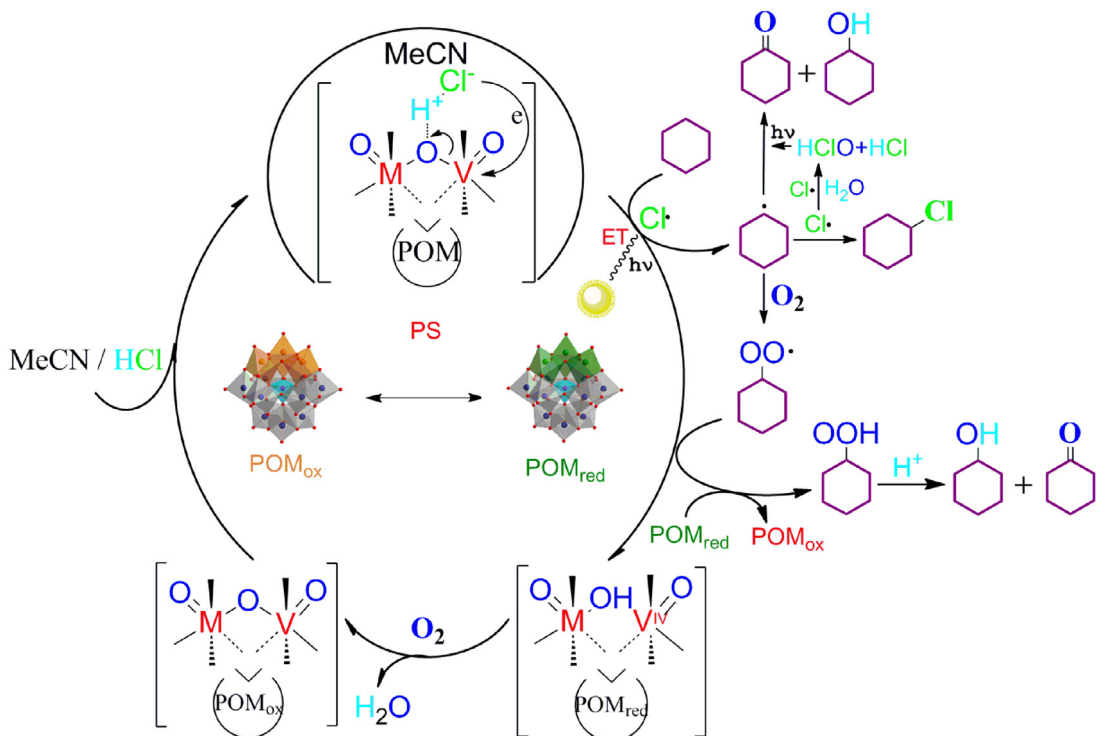


**Fig. 14.** Mass spectra of cyclohexanol (A) and cyclohexanone (B) obtained from TBAPMoV<sub>3</sub>-photocatalyzed cyclohexane oxidation by O<sub>2</sub> in the presence of HCl and H<sub>2</sub><sup>18</sup>O.



**Scheme 2.** proposed photo-catalytic mechanism.

inert N<sub>2</sub> and without water. The free radical trapping agent DMPO can drastically hamper the present photo-reaction. And the additive water can significantly restrain the chlorinated reaction and participate cyclohexane oxidation. The following sequence reactions initiated by the Cl<sup>-</sup> can lead to the formation of oxygenated products (KA oil) and chlorocyclohexane, as well as the regeneration of such PA species. This raises the one question, the formed cyclohexyl radical would react with Cl atom as well as O<sub>2</sub> since bond strength of C–Cl bond (330 KJ/mol) is slightly weaker than that of C–O (350–380 KJ/mol) [60]. How is it possible to yield much lower chlorocyclohexane than KA oil in the present reaction system? We believe that another pathway to generate KA oil should exist in the present photo-oxidation and be relative to the participation of water and Cl atoms, as proposed as follows: the additive water easily reacts with the molecular chlorine Cl<sub>2</sub> generated by the combination of two Cl atoms to generate HCl and HClO, followed by a decomposition of HClO by visible light to generate an active O atom and the latter can oxidize cyclohexane or cyclohexyl

radical to form cyclohexanol and especially cyclohexanone, leading to significantly decreased the chlorinated products and improve cyclohexanone selectivity, as supported by the above reaction and especially H<sub>2</sub><sup>18</sup>O isotope tracing results.

#### 4. Conclusion

In summary, we have found that the vanadium-substituted POMs can interact with HCl to form a photoactive species (PA, POM-(VOHM)<sup>+</sup>Cl<sup>-</sup>) in the participation of solvent MeCN and the latter should be responsible for the present photo-catalytic oxidation. The quaternary ammonium cations- containing POMs in MeCN-HCl-H<sub>2</sub>O media have outstanding advantages in the formation of this PA species and its redox recycling compared to the H<sup>+</sup>-containing counterparts, leading to their high photo-catalytic activities. And the additive water can capture the Cl atoms generated by light-excited PA species to form HClO, and the latter participates the oxidation of cyclohexane, leading to obviously

restrained chlorinated side reactions and improved cyclohexanone selectivity. Having these findings. It is interesting to develop such PA species-based catalytic oxygenation processes for the synthesis of the oxygenated chemicals from other hydrocarbons under light illumination.

## Acknowledgments

We acknowledge the financial support for this work by the National Natural Science Fund of China (21676079, 21546010), the Specialized Research Fund for the Doctoral Program of Higher Education (20124306110005), the Natural Science Fund of Hunan Province (10JJ2007, 14JJ2148), the Innovation Platform Open Fund of Hunan College (11K044, 14K059), the Program for Science and Technology Innovative Research Team in Higher Educational Institutions of Hunan Province and Collaborative Innovation Center of New Chemical Technologies for Environmental Benignity and Efficient Resource Utilization. In addition, we would like to thank professor Y. W. Lin and associate professor J. He of the laboratory of Protein Structure and Function of University of South China for their help in the EPR experiment.

## Appendix A. Supplementary data

Supplementary data associated with this article can be found, in the online version, at <http://dx.doi.org/10.1016/j.apcatb.2017.05.027>.

## References

- [1] R.A. Sheldon, J.K. Kochi, *Metal-Catalyzed Oxidation of Organic Compounds*, Vol. 2 and 11, Academic Press, New York, 1981.
- [2] H.H. Szmant, *Organic Building Blocks of the Chemical Industry*, Wiley, New York, 1989.
- [3] G.W. Parshall, S.D. Ittel, *Homogenous Catalysis*, vol. 10, 2nd ed., Wiley, New York, 1992.
- [4] D.L. Vanoppen, D.E. De Vos, M.J. Genet, P.G. Rouxhet, P.A. Jacobs, *Angew. Chem. Int. Ed. Engl.* 34 (1995) 560–563.
- [5] B.C. Hu, W.Y. Zhou, D.S. Ma, Z.L. Liu, *Catal. Commun.* 10 (2008) 83–85.
- [6] B.P.C. Hereijgers, B.M. Weckhuysen, *J. Catal.* 270 (2010) 16–25.
- [7] (a) G.B. Shul'pin, M.M. Kats, *React. Kinet. Catal. Lett.* 41 (1990) 239–243; (b) G.B. Shul'pin, A.N. Druzhinina, *Mendeleev. Commun.* 2 (1992) 36–37; (c) G.B. Shul'pin, G.V. Nizova, Y.N. Kozlov, *New J. Chem.* 20 (1996) 1243–1256.
- [8] R. Amadelli, M. Bregola, E. Polo, V. Carassiti, A. Maldotti, *J. Chem. Soc. Chem. Commun.* (1992) 1355–1357.
- [9] H. Sun, F. Blatter, H. Frei, *J. Am. Chem. Soc.* 118 (1996) 6873–6879.
- [10] C. Tanielian, *Coordin. Chem. Rev.* 178–180 (1998) 1165–1181.
- [11] M.A. Gonzalez, S.G. Howell, S.K. Sikdar, *J. Catal.* 183 (1999) 159–162.
- [12] Y. Shiraishi, Y. Teshima, T. Hirai, *J. Chem. Soc. Chem. Commun.* 5 (2005) 4569–4571.
- [13] K. Shimizu, Y. Murata, A. Satsuma, *J. Phys. Chem. C* 111 (2007) 19043–19051.
- [14] (a) W.F. Wu, X.L. He, Z.F. Fu, Y.C. Liu, Y.L. Wang, X.L. Gong, X.L. Deng, H.T. Wu, Y.H. Zou, N.Y. Yu, D.L. Yin, *J. Catal.* 286 (2012) 6–12; (b) W.F. Wu, Z.F. Fu, S.P. Tang, S. Zou, X. Wen, Y. Meng, S.B. Sun, J. Deng, Y.C. Liu, D.L. Yin, *Appl. Catal. B: Environ.* 164 (2015) 113–119.
- [15] I.V. Kozhevnikov, *Chem. Rev.* 98 (1998) 171–198.
- [16] N. Mizuno, M. Misono, *Chem. Rev.* 98 (1998) 199–218.
- [17] R. Neumann, *Inorg. Chem.* 49 (2010) 3594–3601.
- [18] R. Neumann, M. Levin, *J. Am. Chem. Soc.* 114 (1992) 7278–7286.
- [19] (a) A.M. Khenkin, R. Neumann, *Angew. Chem. Int. Ed.* 39 (2000) 4088–4090; (b) A.M. Khenkin, L. Weiner, Y. Wang, R. Neumann, *J. Am. Chem. Soc.* 123 (2001) 8531–8542.
- [20] L. Eberson, *Adv. Phys. Org. Chem.* 18 (1982) 79–185.
- [21] (a) P. Mars, D.W. van Krevelen, *Chem. Eng. Sci.* 3 (1954) 41–59; (b) C.N. Satterfield, *Heterogeneous Catalysis in Practice*, McGraw-Hill, New York, 1980.
- [22] E. Papacostantinou, *Chem. Soc. Rev.* 18 (1989) 1–13.
- [23] L. Xu, Y. Wang, X. Yang, X. Yu, Y. Guo, J.H. Clark, *Green Chem.* 10 (2008) 746–755.
- [24] G. Marcì, E. García-López, L. Palmisano, *Eur. J. Inorg. Chem.* 1 (2014) 21–35.
- [25] M.D. Ward, J.F. Brazdil, R.K. Grasselli, *J. Phys. Chem.* 88 (1984) 4210–4213.
- [26] C.L. Hill, D.A. Bouchard, *J. Am. Chem. Soc.* 107 (1985) 5148–5157.
- [27] K. Nomiya, Y. Sugie, T. Miyazaki, M. Miwa, *Polyhedron* 5 (1986) 1267–1271.
- [28] R.F. Renneke, C.L. Hill, *J. Am. Chem. Soc.* 108 (1986) 3528–3529.
- [29] M.A. Fox, R. Cardona, E. Gaillard, J. Am. Chem. Soc. 109 (1987) 6347–6354.
- [30] A.M. Khenkin, L. Weiner, R. Neumann, *J. Am. Chem. Soc.* 127 (2005) 9988–9989.
- [31] C.L. Hill, D.A. Bouchard, M. Kadkhodayan, M.M. Williamson, J.A. Schmidt, E.F. Hilsinski, *J. Am. Chem. Soc.* 110 (1988) 5471–5419.
- [32] I.V. Kozhevnikov, *Catalysis by Polyoxometalates*, Wiley, Chichester England, 2002.
- [33] S.S. Wang, G.Y. Yang, *Chem. Rev.* 115 (2015) 4893–4962.
- [34] S.P. Tang, W.F. Wu, Z.H. Fu, S. Zou, Y.C. Liu, H.H. Zhao, S.R. Kirk, D.L. Yin, *ChemCatChem* 7 (2015) 2637–2645.
- [35] J.L. She, Z.H. Fu, J.W. Li, B. Zeng, S.P. Tang, W.F. Wu, H.H. Zhao, D.L. Yin, S.R. Kirk, *Appl. Catal. B: Environ.* 182 (2016) 392–404.
- [36] M. Akimoto, H. Ikeda, A. Okabe, E. Echigoya, *J. Catal.* 89 (1984) 196–208.
- [37] W.W. Guo, Z. Luo, H.J. Lv, C.L. Hill, *ACS. Catal.* 4 (2014) 1154–1161.
- [38] G.B. Shul'pin, T. Sooknoi, L.S. Shul'pina, *Petrol. Chem.* 48 (2008) 36–39.
- [39] J. Jian, K. You, Q. Luo, H. Gao, F.F. Zhao, P. Liu, Q.H. Ai, H. Luo, *Ind. Eng. Chem. Res.* 55 (2016) 3729–3735.
- [40] Y. Zhang, Z. Du, E. Min, *Catal. Today*, 93 (2004) 327–332.
- [41] D. Casarini, G. Centi, P. Jiru, V. Lena, Z. Tvaruzkova, *J. Catal.* 143 (1993) 325–344.
- [42] T. Ilkenhans, B. Herzog, T. Braun, R. Schlögl, *J. Catal.* 153 (1995) 275–292.
- [43] N.A. Alekar, S.B. Halligudi, R. Rajani, S. Gopinathan, C. Gopinathan, *React. Kinet. Catal. Lett.* 72 (2001) 169–176.
- [44] E.B. Wang, C.W. Hu, L. Xu, *Introduction of Polyacids Chemistry*, Chemical Industry Press, Beijing, 1998.
- [45] A.J. Esswein, D.G. Nocera, *Chem. Rev.* 107 (2007) 4022–4047.
- [46] M.J. Watras, A.V. Teplyakov, *J. Phys. Chem. B* 109 (2005) 8928–8934.
- [47] K.T.V. Rao, B. Haribalu, P.S.S. Prasad, N. Lingaiah, *Green. Chem.* 15 (2013) 837–846.
- [48] T. Mazari, C.R. Marchal, S. Hocine, N. Salhi, C. Rabia, *J. Energy. Chem.* 18 (2009) 319–324.
- [49] K. Malka, J. Aubard, M. Delamar, V. Vivier, M. Che, C. Louis, *J. Phys. Chem. B* 107 (2003) 10494–10505.
- [50] J.K. Lee, J. Melsheimer, S. Berndt, G. Mestl, R. Schlögl, K. Köhler, *Appl. Catal. A: Gen.* 214 (2001) 125–148.
- [51] M.A. Leparulo-Loftus, M.T. Pope, *Inorg. Chem.* 26 (1987) 2112–2120.
- [52] L. Pettersson, I.G. Andersson, A. Selling, J.H. Grate, *Inorg. Chem.* 33 (1994) 982–993.
- [53] (a) T. Okuhara, N. Mizuno, M. Misono, *Appl. Catal. A: Gen.* 222 (2001) 63–77; (b) C.R. Waidmann, A.G. DiPasquale, J.M. Mayer, *Inorg. Chem.* 49 (2010) 2383–2391.
- [54] P. Schwendt, J. Tatiersky, L. Krivosudský, M. Šimuneková, *Coordin. Che. Rev.* 318 (2016) 135–157.
- [55] J.T. Wang, B.S. Zhang, Y.M. Wang, Q.M. Hu, *Organic Chemistry*, vol. 2, second ed., Nankai University press, Tianjing, 2002.
- [56] N.D. Yordanov, K. Ranguelova, *Spectrochim. Acta. Part A* 58 (2002) 1171–1180.
- [57] T.T. Zhang, J.F. Jia, H.S. Wu, *J. Phys. Chem. A* 114 (2010) 12251–12257.
- [58] W.F. Wu, Z.H. Fu, X. Wen, Y.J. Wang, S. Zou, Y. Meng, Y.C. Liu, S.R. Kirk, D.L. Yin, *App. Catal. A: Gen.* 469 (2014) 483–489.
- [59] K. Takaki, J. Yamamoto, K. Komeyama, T. Kawabata, K. Takehira, *Bull. Chem. Soc. Jpn.* 77 (2004) 2251–2255.
- [60] M.B. Smith, *March's Advanced Organic Chemistry: Reactions, Mechanisms, and Structure*, vol. 2, John Wiley & Sons Press, 2012.
- [61] A.M. Khenkin, A. Rosenberger, R. Neumann, *J. Catal.* 92 (1999) 82–91.
- [62] G.R. Buettner, *Free Radicals. Biol. Med.* 3 (1987) 259–303.